NASA TECHNICAL
MEMORANDUM

NASA TM X-64513

ATMOSPHERIC EFFECTS ON WAVE PROPAGATION AT 10.6 MICRONS

By William E. Webb*, Kermit H. George**,
and Peter Marrero
Astrionics Laboratory

April 30, 1970

* Summer employee, visiting professor program; present address: University of Alabama, Tuscaloosa, Alabama.

** Graduate student summer program; present address: University of Alabama, Tuscaloosa, Alabama.

NASA

George C. Marshall Space Flight Center
Marshall Space Flight Center, Alabama

MSFC - Form 3190 (September 1968)

TECHNICAL REPORT STANDARD TITLE PAGE

1. REPORT NO.	2. GOVERNMENT ACCESSION NO.	3. RECIPIENT'S CATALOG NO.
TM X-64513		

4. TITLE AND SUBTITLE	5. REPORT DATE
Atmospheric Effects on Wave Propagation at 10.6 Microns	April 30, 1970
	6. PERFORMING ORGANIZATION CODE
7. AUTHOR(S) William E. Webb, Kermit H. George, and Peter Marrero	8. PERFORMING ORGANIZATION REPORT #
9. PERFORMING ORGANIZATION NAME AND ADDRESS George C. Marshall Space Flight Center Marshall Space Flight Center, Alabama 35812	10. WORK UNIT NO.
	11. CONTRACT OR GRANT NO.
	13. TYPE OF REPORT & PERIOD COVERED Technical Memorandum
12. SPONSORING AGENCY NAME AND ADDRESS	14. SPONSORING AGENCY CODE

15. SUPPLEMENTARY NOTES

Prepared by the Astrionics Laboratory

16. ABSTRACT

A CO_2 laser communications system using optical heterodyne detection has been operated over a 3.2-km path at the Marshall Space Flight Center. Both scintillation and heterodyne measurements were made for varying receiver apertures and under varying atmospheric conditions. The results have been analyzed to determine the statistical distribution function for the intensity fluctuations, the atmospheric structure constant, and the power spectrum. Signal-to-noise measurements indicate that reliable heterodyne communications are possible even under deep scintillation conditions.

17. KEY WORDS	18. DISTRIBUTION STATEMENT
Optical Communications CO_2 Laser Atmospheric Propagation Scintillation	

19. SECURITY CLASSIF. (of this report)	20. SECURITY CLASSIF. (of this page)	21. NO. OF PAGES	22. PRICE
Unclassified	Unclassified	38	$3.00

MSFC - Form 3292 (May 1969)

TABLE OF CONTENTS

LIST OF ILLUSTRATIONS

LIST OF TABLES

TECHNICAL MEMORANDUM X-64513

ATMOSPHERIC EFFECTS ON WAVE PROPAGATION AT 10.6 MICRONS

SUMMARY

A CO_2 laser communications system using optical heterodyne detection has been operated over a 3.2-km path at the Marshall Space Flight Center. Both scintillation and heterodyne measurements were made for varying receiver apertures and under varying atmospheric conditions. The results have been analyzed to determine the statistical distribution function for the intensity fluctuations, the atmospheric structure constant, and the power spectrum. Signal-to-noise measurements indicate that reliable heterodyne communications are possible even under deep scintillation conditions.

INTRODUCTION

Although the effects of atmospheric turbulence on optical propagation have been widely investigated, both experimentally and theoretically [1,2], the amount of data available for 10.6-micron laser beams is minimal. Especially lacking are data concerning the effects of the atmosphere on heterodyne detection at this wavelength. Furthermore some of the existing data do not seem to agree closely with the theoretical predictions. Recently two investigators [3,4] reported deviations of the intensity fluctuations from the log-normal distribution predicted by the accepted theory, while other investigators [5,6] reported preliminary results that tend to confirm the log-normal distribution.

The scintillation and heterodyne signal-to-noise ratios were investigated for a CO_2 laser beam propagated for a distance of 3.2 km through the atmosphere. Both scintillation and heterodyne measurements have been made for a variety of receiving aperture sizes ranging from 2 cm to 10 cm.

EXPERIMENTAL MEASUREMENTS

The experimental measurements were made during the summer of 1969 at the Marshall Space Flight Center's optical range located at Redstone Arsenal, Alabama.

The transmitting system was located in an astronomical observatory on the crest of Madkin Mountain. The receiving and recording systems were located in the Astrionics Laboratory complex in a special building equipped with a large mirror periscope so that the optical equipment could be conveniently placed on ground level yet have a clear optical path to the mountain. The height of the periscope was about 4.5 m above ground level. The optical path extended in a southwesterly direction for a distance of 3.2 km. The transmitter was about 220 m above the receiver so that the optical path was at a 4-degree angle with the horizontal. Except for a few small buildings and a parking lot paved with bituminous material, the optical path lay mostly over wooded terrain.

The transmitter and receiver were constructed for Marshall Space Flight Center by the Honeywell Corporation and have been described in the literature [7]. The laser transmitter consisted of a 2-W CO_2 laser with a 10-cm off-axis cassegrainian collimator. The laser was stabilized by use of a temperature-controlled cervit cavity. The laser could be frequency modulated by driving one of the cavity mirrors mounted on a piezoelectric pusher. The transmitting unit contained a mechanical chopper that was originally intended to be used for alignment purposes. The receiver consisted of a 10-cm aperture off-axis cassegrainian telescope, a local oscillator similar to the transmitter laser, combining optics, and a mercury-doped cadmium telluride detector. The receiver employed typical FM receiver electronics, except that the automatic frequency control feedback drove one of the piezoelectric pushers which accomplished frequency locking of the laser to the incoming signal.

It was necessary to measure the laser and amplifier noise of the system to ensure that it would not have a significant effect on measurements made through the atmosphere. Noise measurements were made with the transmitter and receiver placed a few meters apart, and also with them placed 100 m apart at opposite ends of an enclosed tunnel which was 1 m in diameter. This noise was found to be sufficiently low so that it would be negligible compared to the expected scintillation. The linearity of the mercury cadmium telluride detector was also investigated at this time. For incident power levels less than 300 mW, the detector output was found to be quite linear.

Alignment of the system over the 3.2-km path proved to be a difficult task. In the first attempt to align the system, a 60-power telescope mounted on the transmitter's case was accurately boresighted with the laser beam. The transmitting unit was then aimed at the periscope. This technique was not successful because of problems with maintaining a good boresight. The second method employed to align the system involved the use of two visible lasers. To align the transmitter, a 12-mW argon laser was placed adjacent to the receiver unit. The bright beam could easily be detected by the eye at the transmitting terminal. The argon laser was moved until its beam was intercepted by the objective of the transmitter unit. The optical system of the transmitter was adjusted so that the visible laser was focused onto the output aperture of the CO_2 laser. The output of the CO_2 laser was then made to coincide with the argon beam at two points in the optical system. The receiver was aligned in a similar manner. A small He-Ne laser was mounted with a boresighted telescope on a tripod located adjacent to the transmitter unit. The He-Ne laser was then aimed until its reflection could be seen from a corner reflector located in the periscope at the receiver site. The receiver optics were then appropriately adjusted to focus the He-Ne beam onto the detector in the receiver. This provided very close alignment for the 10.6-micron beam.

To obtain the actual intensity variation of the infrared laser light, it was necessary to compensate for the background light caused by the sun's reflection from the observatory dome by chopping the beam with the 90-Hz chopper in the transmitter. The local oscillator in the receiver was turned off so that only light from the transmitter was incident on the detector. The output of the detector was amplified and recorded directly with an Amperex 14-channel FM instrumentation tape recorder. Thus, the recorded signal consisted of an amplitude modulated square wave whose amplitude was proportional to the instantaneous power being received.

When recording scintillation data, the output of the Hg-Cd-Te detector was capacitively coupled to a variable-gain amplifier whose output drove the analog tape recorder. The analog tape recorder was carefully checked and its linear range of operation was determined. The input and output of the recorder had to be continuously monitored with an oscilloscope to assure that the input level was not driving the recorder out of its linear range. The input voltage was critical since the recorder's linear operating range was only ± 1 volt. The measurements did not exceed ± 0.5 volt.

Signal-to-noise measurements were made of heterodyne detection at the receiver by extracting the 10-MHz beat note between the received signal

and the local oscillator after it had passed through one stage of IF amplification. The signal was detected with a simple diode circuit and the resulting voltage was recorded on magnetic tape. In addition, the transmitter was frequency modulated at 1 kHz and the audio output signal was recorded at the receiver.

Both scintillation and signal-to-noise measurements were made with different size receiver apertures. The aperture sizes had to be changed rapidly over a short time interval to ensure that atmospheric conditions remained constant. Five apertures of 2, 4, 6, 8, and 10 cm in diameter were used.

Twelve channels of each analog magnetic tape were used for data and the other two channels were used for identification and timing. The identification channel was divided into 33 equally spaced time segments, each marked with an audible tone. The data runs were recorded in the marked time slots so that they could be easily located for later reference. A standard AMR-5 binary timing code was recorded on the other channel to be used by the analog-to-digital converter.

Approximately 750 observations of scintillation were made at all hours of the day and under as wide a variety of weather conditions as possible. Each observation consisted of about 90 seconds of recorded data from which a 60-second segment near the center of each run was selected for processing. The run number, tape number, time of day, temperature, humidity, wind speed, and general weather conditions were recorded for each observation.

ANALOG-TO-DIGITAL CONVERSION

Before processing, the experimental data had to be converted to a digital form suitable for computer input. The very large quantity of data collected necessitated electronic conversion to digital magnetic tape that could then be read directly into the computer.

The analog-to-digital conversion was accomplished on the MSFC Computation Laboratory's analog-to-digital stand, the digitization being controlled by the recorded timing channel. Five data channels were digitized simultaneously. These five channels were sampled alternately at a rate of 5000 samples per second (1000 samples per second from each channel), and the output was recorded on a 7-channel digital tape in a multiplexed format.

Data Reduction

To reduce the data, a program has been written for the IBM 360 Model 50 computer. The principal problems that were encountered in writing this program concerned formating the data for the computer and extracting the amplitude of the square wave. The latter proved to be somewhat difficult since the sampling rate during digitization could not be accurately synchronized with the period of the square wave. The sampling rate of 1 kHz and the chopping rate of 90 Hz should yield approximately 10 samples per cycle of the square wave. In actuality, the number of samples per cycle varied between 10 and 12 because the sampling rate was not an integral multiple of the square-wave frequency. It was therefore necessary to design a program that would determine whether a particular data point was a base point (i.e., from the part of the square wave when the laser beam was blocked by the chopper) or a signal point (when power was being received from the laser beam). The problem was further compounded because the rise and fall times of the square wave were nonnegligible so that about 1 percent of the data points was sampled during the switching transient and should therefore be discarded. Furthermore, some of the data contained an occasional noise spike that should be eliminated. It was decided that the elimination of these spikes would not adversely affect the validity of the analysis so provisions for eliminating them were also included in the program.

The program written to divide the data into base and signal points operates basically as follows. One record, containing 2000 characters, is read from magnetic tape. These 2000 characters represent 200 sample values from each of 5 data channels. Each sample value is a 10-bit binary number plus sign bit occupying two tape characters. The 400 characters corresponding to the channel being analyzed are converted to internal floating point format and are stored in an array. A second record is read from the tape, then converted and stored in a second array. To begin the analysis, 20 data points from the first of the array are selected and the maximum and minimum are found. Two limits, L_1 and L_2, are then set by the relations

$$L_1 = A_{max} - P_1(A_{max} - A_{min}) \tag{1}$$

$$L_2 = A_{min} + P_2(A_{max} - A_{min}) \tag{2}$$

where A_{max} and A_{min} are the maximum and minimum of the first 20 points and P_1 and P_2 are constants between zero and one-half. Since the signal

was inverted when it was recorded on analog tape, the baseline is greater than the signal; hence, a particular point greater than L_1 is considered a base point. If it is less than L_2, it is considered a signal point. Points lying between L_1 and L_2 are assumed to be from the transient portion of the waveform and are neglected.

The computer is programed to take each point successively and to determine if it is a base point, a signal point, or neither. As a preliminary to processing, the first 20 points are scanned and the beginning of a baseline segment of the waveform is found. Then new limits are set on the next 15 points and they are scanned and grouped into 3 arrays, a baseline segment, a signal segment, and a second baseline segment. Each array may contain up to 7 points. At this time the amplitude of the square wave is computed for the group of signal points (as will be described later) and stored. The second group of base points is transferred into the first array, new limits are set using the next 10 data points, a new group of signal and base points are found to fill the second and third arrays, and finally their amplitudes are computed. This process is continued until the 200 points from the first record have been used. At this time the 200 points from the second tape record are transferred into the array formerly occupied by the first record and a third record is read from tape. Processing then continues until as much of the data as desired have been processed. Usually, 10 000 data points were used for the analysis although as many as 60 000 could be used.

Data Processing Irregularities

As previously mentioned, several irregularities in the data are possible and a number of checks have been built into the program to provide for them. These checks are as follows:

(1) During the search for either base or signal points, more than 10 consecutive points are found.

(2) After completing a search, less than 3 base or signal points have been found.

(3) More than 3 consecutive points satisfying neither the base nor the signal point critieria are found.

Any of these three conditions indicate that the waveform is departing drastically from a modulated square wave, and appropriate action should be taken. For

conditions (1) and (3) above, the program skips 10 data points, or approximately one cycle of the square wave, and begins processing again. For condition (2) the computation of amplitudes is suppressed and processing continues. As a further check, if the total number of errors in any record exceeds five, the entire record is omitted.

During processing, a record is kept of each time an irregularity was encountered and this information is printed in tabular form at the completion of processing. Clearly, if an excessive number of irregularities occur in a given run, the results of that run must be suspect.

Computation of Amplitudes

After each cycle of the waveform has been processed to divide the data points into base points and signal points, the amplitude is computed. Three methods for computing the amplitude have been tried. The first method took the baseline for a group of signal points as the average of all the points in the group of base points preceding it and the one following it; that is, the background during the half-cycle in which the laser beam intensity was recorded is taken as the average background recorded during the half-cycle immediately preceding the signal and the half-cycle immediately following it. This average baseline was subtracted from each signal point and the difference taken as the amplitude of the laser beam at that instant.

The second type of amplitude calculation considered was to reconstruct the baseline during the period when the signal was recorded by fitting a least-mean-square curve to the baseline points on either side. This method gave very erratic results and was abandoned.

The third method consisted of taking the difference in the first signal point in a group and the last base point preceding it as an amplitude. The difference in the last signal point in the group and the first base point following it gives a second amplitude. This method gives only two amplitudes per cycle but has the advantage that they are evenly spaced.

The final computer program contained both the first- and third-type amplitude calculation, the one to be used being selected by a parameter read during execution. An option is also provided that will either store all amplitudes along with the time at which the amplitude occurred or will, instead of storing the amplitude, count the number of times an amplitude lying in a given range occurs. The former yields received beam intensity as a function

of time while the latter gives the probability density function for the intensity fluctuations. Either is saved for whatever analysis one wishes to perform on the data.

Program Checkout and Adjustment of Parameters

To test the program, a segment of data was printed from the magnetic tape and was inspected. Each data point was classified as either a signal point, a base point, or a bad point from the transient portion of the waveform. This classification was purely subjective; yet in inspecting the data there were usually no questions as to how a particular point should be categorized. The same data were then fed into the computer. Print statements were added to the program to list each point and indicate how the computer classified it. The program was run several times varying the parameters P_1 and P_2 [equations (1) and (2)] between runs and the results were compared with the subjective analysis. Data containing "bad places" were also processed and the results were compared with our judgment as to whether a segment should be omitted. On the basis of these comparisons, the parameters P_1 and P_2 were set at 0.05 and 0.10, respectively; that is, a point within 5 percent of the maximum base point or 10 percent of the minimum signal point would be retained while points between these limits were discarded. These limits seemed to allow the computer to make very nearly the same decisions as we would have made had we analyzed the data by hand.

Because of the statistical nature of the analysis, the results will not be appreciably affected if a few points are discarded as bad that should have been retained. Preliminary analysis of the data seems to confirm that the results are not too sensitive to small changes in the values of the limits.

Calculations of the Scintillation Statistics

The final segment of the data analysis program accepts the probability density function generated for the intensity fluctuations and computes the scintillation statistics. The program computes and lists the class mark for the intensity and the corresponding value of the log-amplitude defined by

$$\ell_i = \frac{1}{2} \ln (I_i / \overline{I}) \qquad (3)$$

where ℓ_i and I_i are the log-amplitude and the intensity for the ith class interval, and $\bar{I}$ is the mean intensity. The frequency for each class and the cumulative probability are also listed.

It has been customary in the literature to test the hypothesis of log-normality of scintillation data by plotting the cumulative probability function of the log-amplitudes against a "probability scale" such that if the data are log-normal, the resulting curve will be a straight line. Not only is this procedure not a very sensitive test of a statistical distribution but it is also very time consuming when a large quantity of data are to be processed. We have therefore included in the program a chi-square test on both a normal and a log-normal distribution function. These tests provide a quick and sensitive means of testing the hypothesis of log-normal scintillation.

The statistical analysis routine also computes the mean, standard deviation, skewness, and kurtosis for both the intensity distribution and the log-amplitude distribution. From the standard deviation of the log amplitudes, the atmospheric structure constant has been computed. The skewness and kurtosis were also computed to give an additional check on log-normality.

ATMOSPHERIC REFRACTIVE – INDEX STRUCTURE CONSTANT

The log amplitude variance $C_\ell(0)$ for a plane wave is given in terms of the atmospheric structure constant C_n by [8].

$$C_\ell(0) = 0.309\, k^{7/6} Z^{11/6} C_n^2 \quad , \tag{4}$$

where k is the wave number and Z is the length of the path through the atmosphere. For a spherical wave, the corresponding expression is

$$C_\ell(0) = 0.124\, k^{7/6} Z^{11/6} C_n^2 \quad . \tag{5}$$

In the preliminary analysis, the finite aperture of the receiver was neglected and it was treated as being negligibly small. Equations (4) or (5) can then be used directly to obtain C_n^2 by noting that the standard deviation of the log-amplitude distribution that was computed is the square root of

$C_\ell(0)$. It is well known however that a finite receiving aperture has the effect of averaging the intensity fluctuation from various parts of the wave front, thereby reducing the variance of the scintillation. This effect has been investigated by Fried [9]. From Figure 2 in Fried's paper, we note that for large scintillation conditions and for the path length and apertures used in our experiment, this effect will be significant.

To allow for aperture averaging, we may use the expressions given by Fried [10], viz.

$$\sigma_s^2 = \left[\frac{\pi}{4} D^2\right]^2 \theta\, C_I(0) \tag{6}$$

where σ_s^2 is the signal variance that corresponds to the square of the standard deviation of the intensity fluctuation, $C_I(0)$ is the irradiance covariance, D is the diameter of the receiving aperture, and θ is an aperture averaging factor given by

$$\theta = \frac{16}{\pi D^2} \int_0^D \rho d\rho \, \frac{\exp[4C_\ell(\rho)]-1}{\exp[4C_\ell(0)]-1} \, H(\rho/D) \quad . \tag{7}$$

$H(\rho/D)$ is the optical transfer function of a circular aperture

$$H(\rho/D) = \cos^{-1}(\rho/D) - (\rho/D)\,[1 - (\rho/D)^2]^{1/2} \tag{8}$$

and $C_\ell(\rho)$ is the log-amplitude covariance given by

$$C_\ell(\rho) = C_\ell(0) \sum_{n=0}^{\infty} \left[a_{11} + b_n \left(\frac{k\rho^2}{4z}\right)\right] \times \left[\left(\frac{k\rho^2}{4z}\right)/(2n)!\right] - 7.53034 \left(\frac{k\rho^2}{4z}\right)^{5/6} \quad . \tag{9}$$

In the last expression a_n and b_n are the expansion coefficients for the modified confluent hypergeometric function ${}_1F_1\left(-\frac{11}{6}; \underline{1}; ix\right)$ and are given by

$$a_o = 1$$
$$b_o = 6.84209 \qquad (10)$$

and the recursion relations

$$a_n = -a_{n-1}\left[(2n - 23/6)(2n - 17/6)/(2n - 1)(2n)\right] \qquad (11a)$$

$$b_n = -b_{n-1}\left[(2n - 17/6)(2n - 11/6)(2n-1)/(2n)(2n + 1)^2\right]. \qquad (11b)$$

With the additional relation that the intensity variance $C_I(0)$ in equation (6) is related to the log variance by

$$C_I(0) = I_o^2\left[\exp[4C_\ell(0)] - 1\right] \qquad (12)$$

equations (6) through (12) specify $C_\ell(0)$ in terms of σ_s^2 and I_o^2. Since I_o and σ_s are just the mean and standard deviation of the received intensity, we may compute $C_\ell(0)$; and then using equation (5), we find the atmospheric structure constant.

Combining the above equations we have

$$\left(\frac{\sigma_s}{I_o}\right)^2 = \pi D^2\left[\exp\left[4C_\ell(0)\right] - 1\right]$$
$$\times \int_o^D \rho d\rho \, \frac{\exp\left[4f\,\frac{4\rho}{4z}\cdot C_\ell(0)\right] - 1}{\exp\left[4\,C_\ell(0)\right] - 1} H(\rho D) \qquad (13)$$

where $f(k\rho/4z)$ is the summation given in equation (9).

Since σ_s/I_o is an experimentally determined constant, equation (13) is an integral equation for $C_\ell(0)$. We have programed the IBM 360 computer to solve equation (13). The technique used is to evaluate the integral in equation (13) for a number of trial values of $C_\ell(0)$ using a fourth-order

Runge-Kutta integration. This gives a table of σ_s/I_o as a function of $C_\ell(0)$. From this table, the value of $C_\ell(0)$ corresponding to the measured value of σ_s/I_o is determined using Lagrange-Hermite interpolation formula.

Scintillation Frequency

It is customary in the literature to describe the frequency of the scintillation in terms of the power spectral density of the log-amplitude fluctuations. Properly, the power spectral density is defined as the Fourier transform of the correlation function of the log amplitudes. Because of the computational complexities involved in calculating this quantity, we have elected to work instead with the spectrum of the intensity fluctuations. Although the intensity spectrum is not as readily comparable to the theory as is the log amplitude, it provides a convenient measure of the bandwidth of the scintillation that can be readily calculated.

In calculating the scintillation spectrum 2^{18} (or 8192) values of the beam intensity were extracted from the raw data using the preprocessing program described previously. These values represent the intensity fluctuations of the beam sampled at a rate of 180 Hz; i.e., every 5.55 ms. In cases where a few data points were discarded because of errors in the preprocessing routine, the omitted points were replaced with either random numbers or with a constant to preserve the temporal relation of the signal. Test of the program indicated that the resulting spectrum is insensitive to the method used to replace these points. Since only data with very few processing errors were analyzed, it is felt that these errors did not affect the final result. After preprocessing, the spectrum of the sampled data was computed using the Cooley-Tukey algorithm [11] for fast Fourier transforms. The resulting spectra were displayed by means of a computer plot routine.

RESULTS

Probability Density Function

The standard method used to determine how closely scintillation data conform to a log-normal distribution is to plot the cumulative probability function of the log amplitudes on a probability scale such that if the data conform, the resulting curve will be a straight line. The same method can be used when testing for the normal case. Since this test would require

considerable time if it were applied to every run, it was necessary to use a test that could be incorporated into a computer program to determine more efficiently the type of distribution each run most closely fit.

The necessary statistical parameters to make this test were calculated in the main program and were retained on punched cards. The skewness was chosen as the parameter to determine the type distribution. This parameter must have a much smaller value for the log-amplitude distribution than for the amplitude distribution if the data are to be considered log-normal. Also the value of the chi-square test for the first should be smaller in proportion to that of the latter by at least an order of magnitude. The reverse of this would be required for a normal fit. We have chosen the skewness as the measure of goodness-of-fit in preference to the chi-square test since chi-square depends upon the number of class intervals in the sample while the skewness does not. The generation of a table of chi-square for all possible number of class intervals would lead to unwarranted additional complexities in the computer program.

To use the skewness as a criterion for categorizing the data, it was necessary to set bounds on its value. Since the lower bound is zero, it was only necessary to determine the largest value that the skewness could attain which would represent a suitable fit. This was accomplished by plotting several graphs of the cumulative probability for runs with values of skewness ranging from very small values (0.02) to larger values (0.79). The chi-square test was examined to ensure that the results of these runs were consistent. A selected number of these graphs are given in Figures 1 through 9. An inspection of these plots will show that the cumulative probability curve becomes nonlinear with increasing values of skewness. On the basis of these graphs, the upper limit placed on the value of skewness was 0.15.

Using this criterion, each of the distributions has been categorized as being either normal, log-normal, or neither. In addition, a category has been included for those distributions that were sufficiently close to both a normal and a log-normal distribution that they could not be distinguished from each other. These runs, which have approximately the same skewness for the amplitude and log-amplitude distributions, have been designated as "both." The number of runs that fall into this category indicate the well-known fact that normal and log-normal distributions differ only in their tails and, hence, are often difficult to distinguish in real data.

The results of this categorization for 196 runs are shown in Table 1. Only runs with a small number of preprocessing irregularities have been

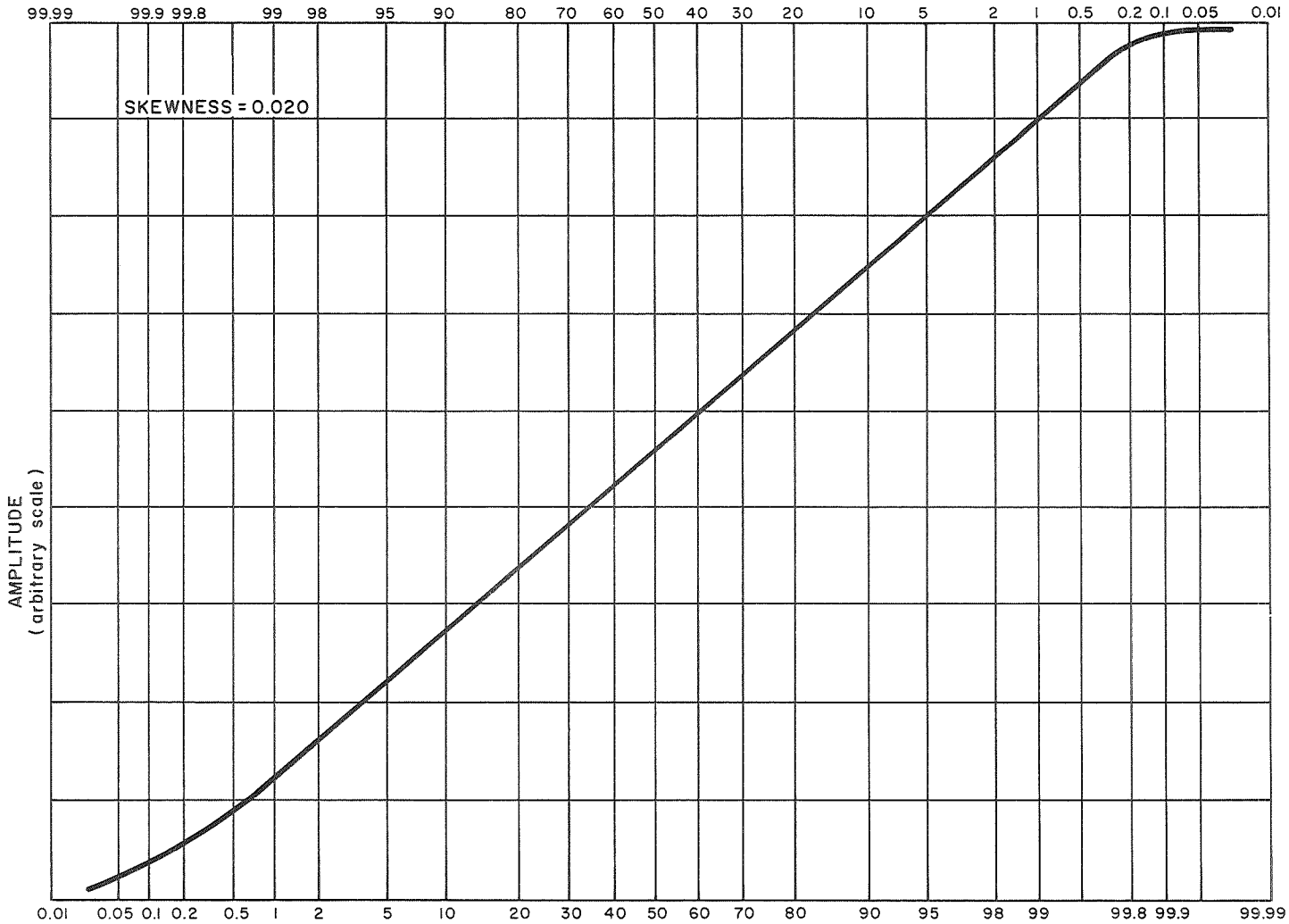

Figure 1. Probability density — skewness = 0.020.

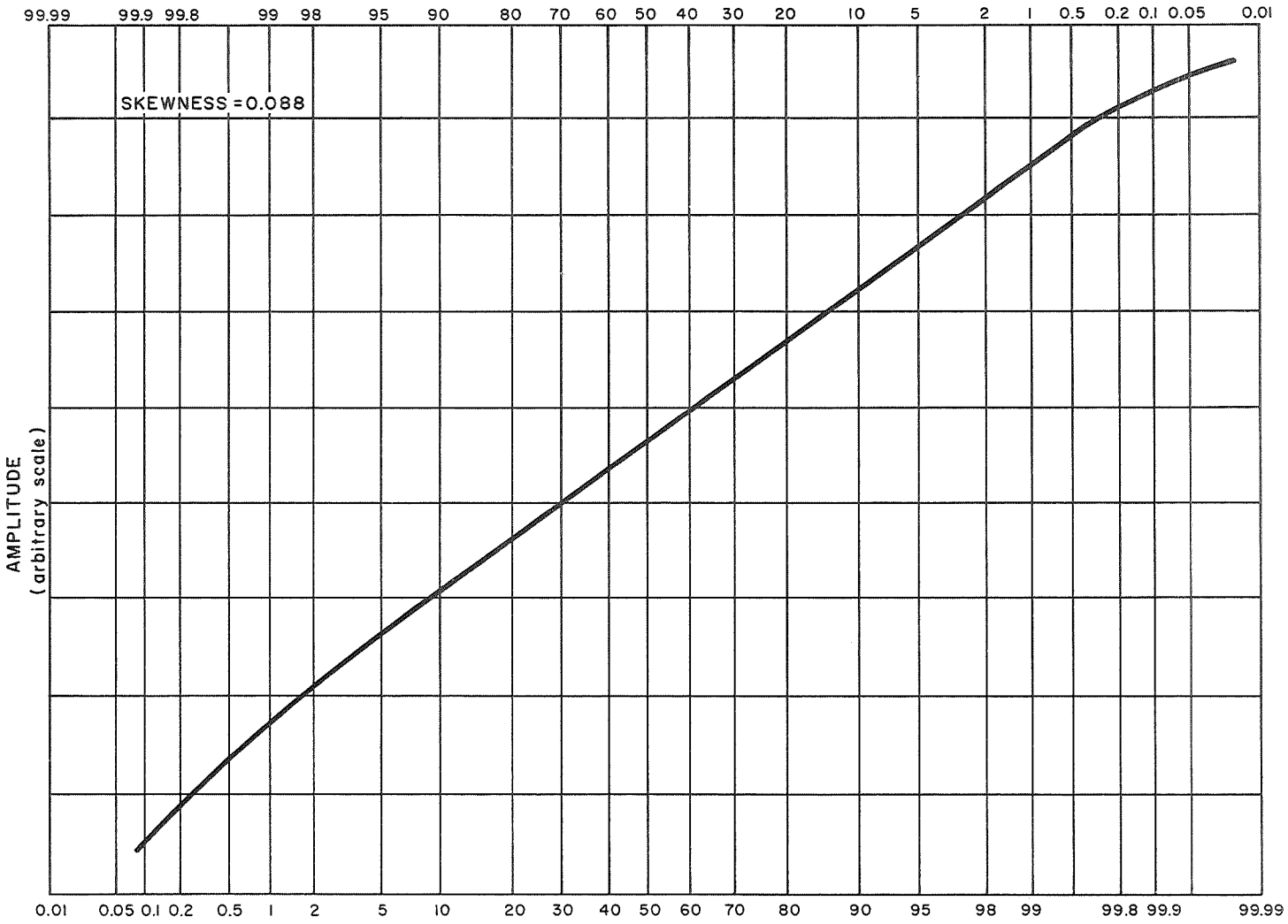

Figure 2. Probability density — skewness = 0.088.

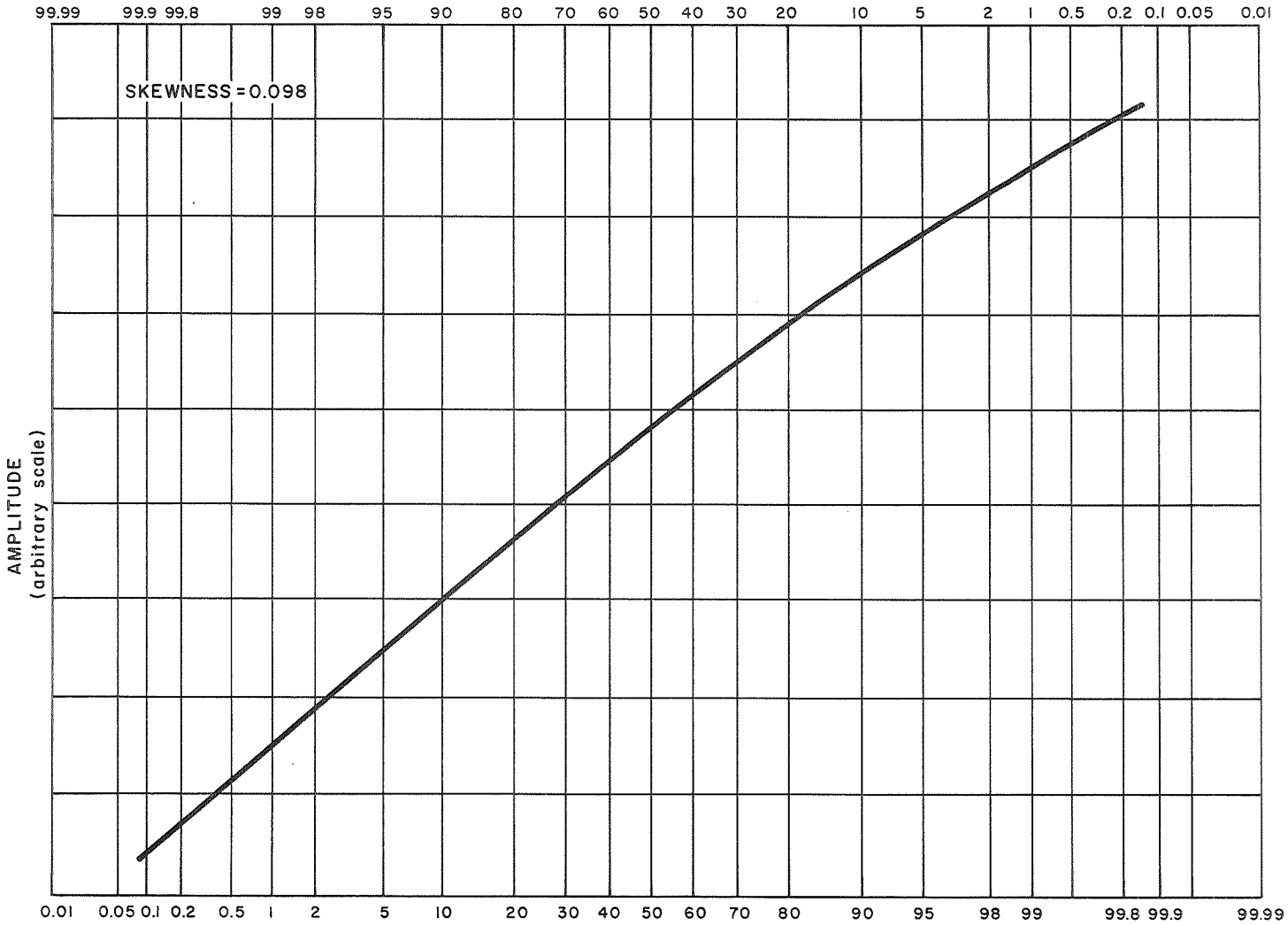

Figure 3. Probability density — skewness = 0.098.

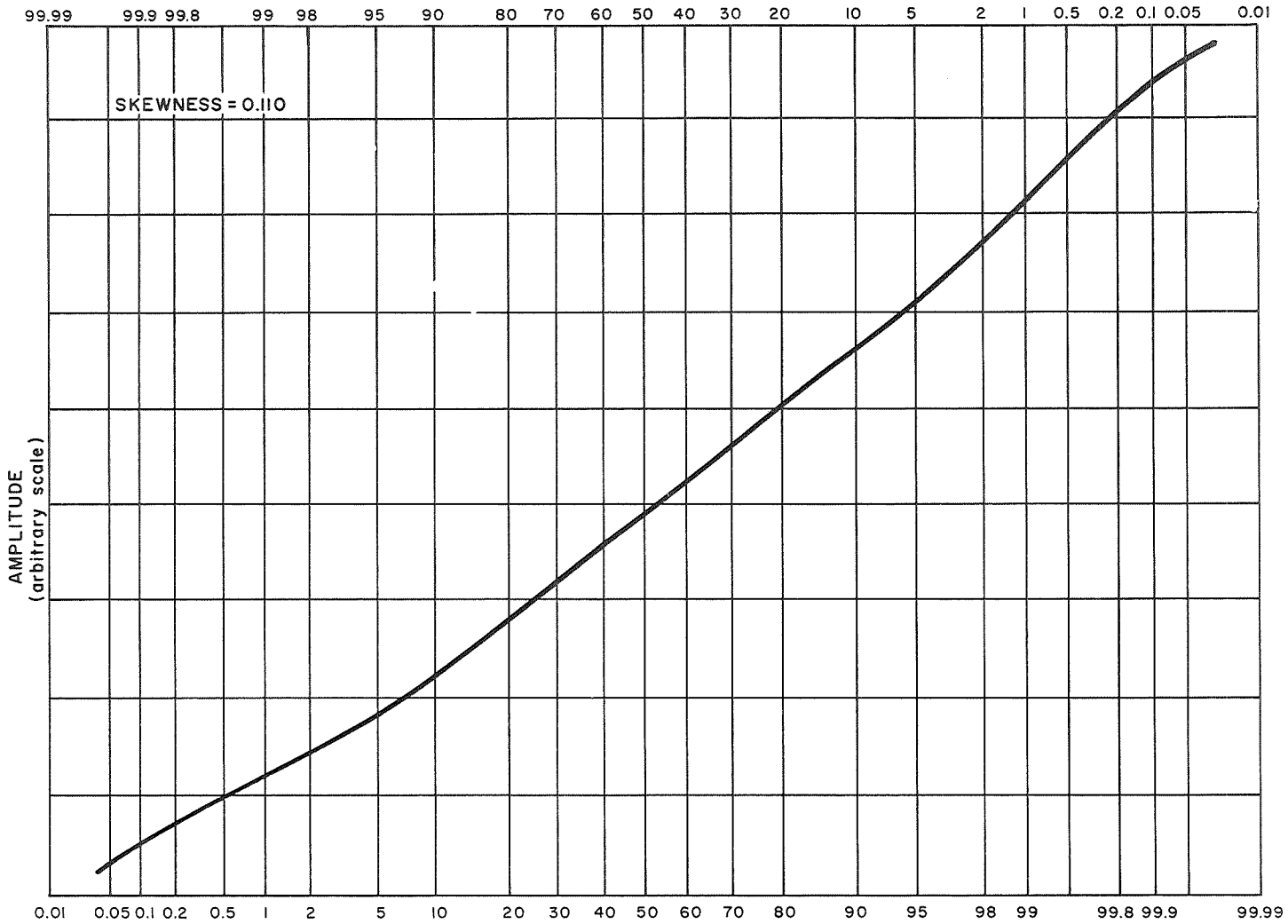

Figure 4. Probability density — skewness = 0.110.

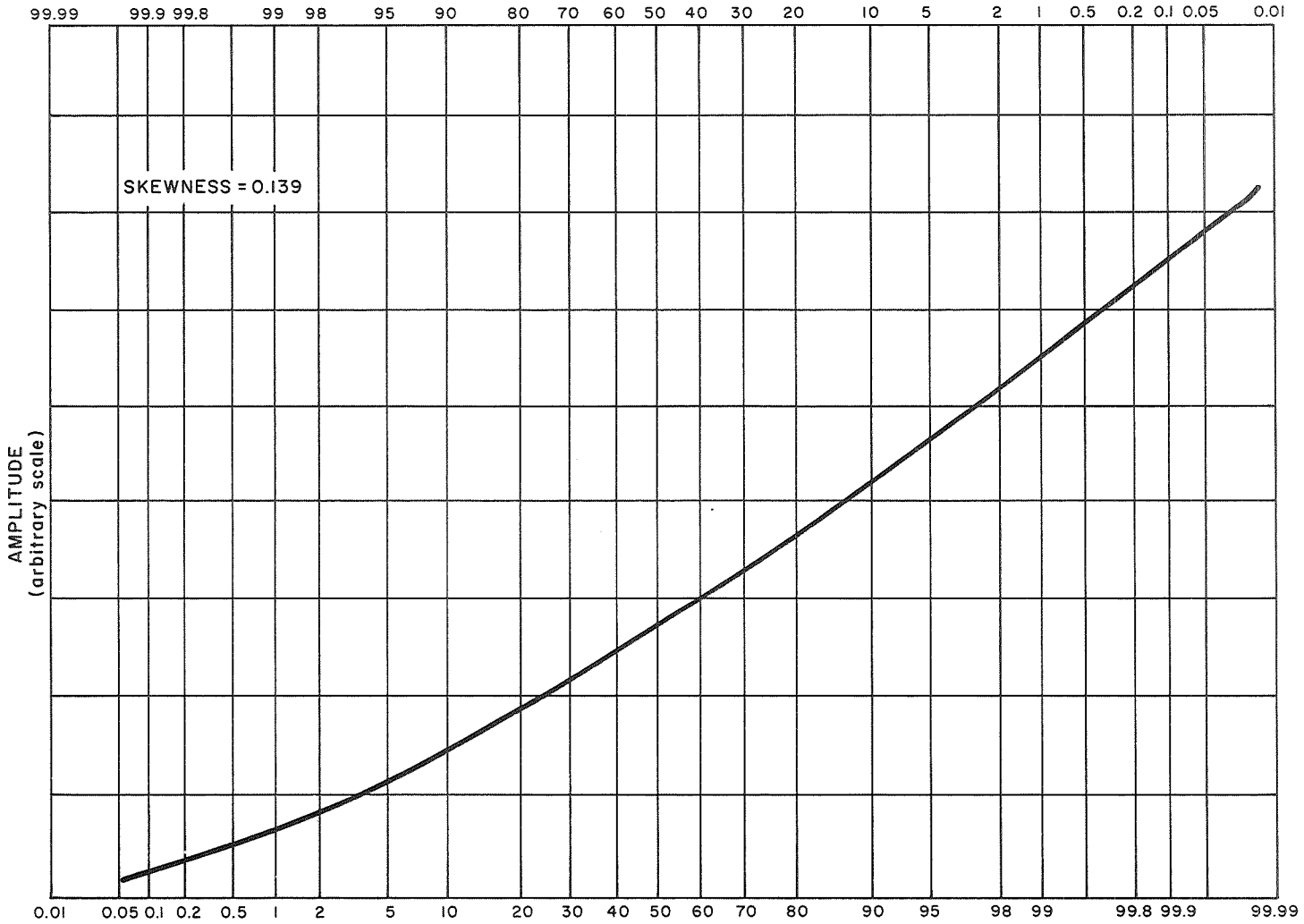

Figure 5. Probability density — skewness = 0.139.

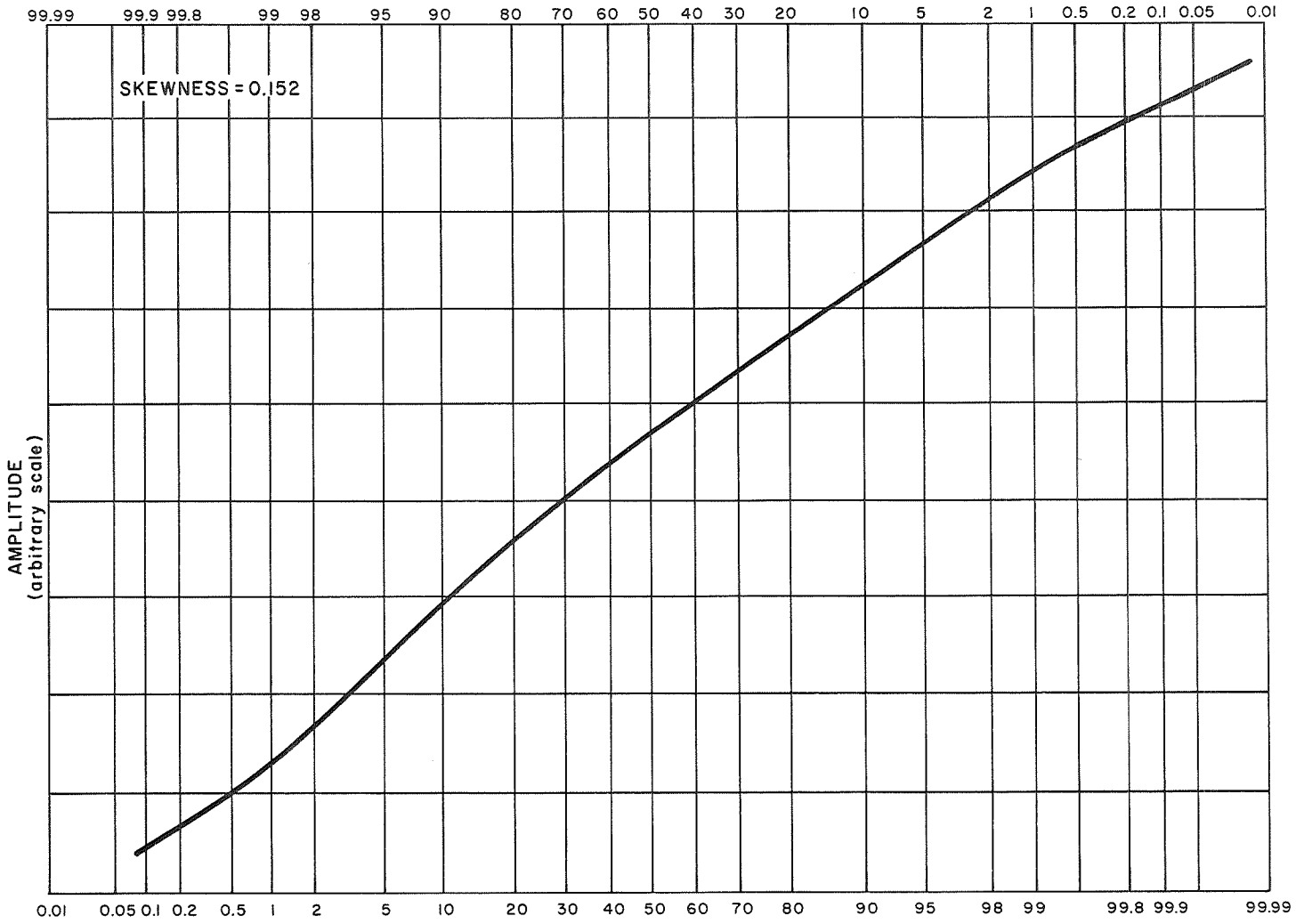

Figure 6. Probability density — skewness = 0.152.

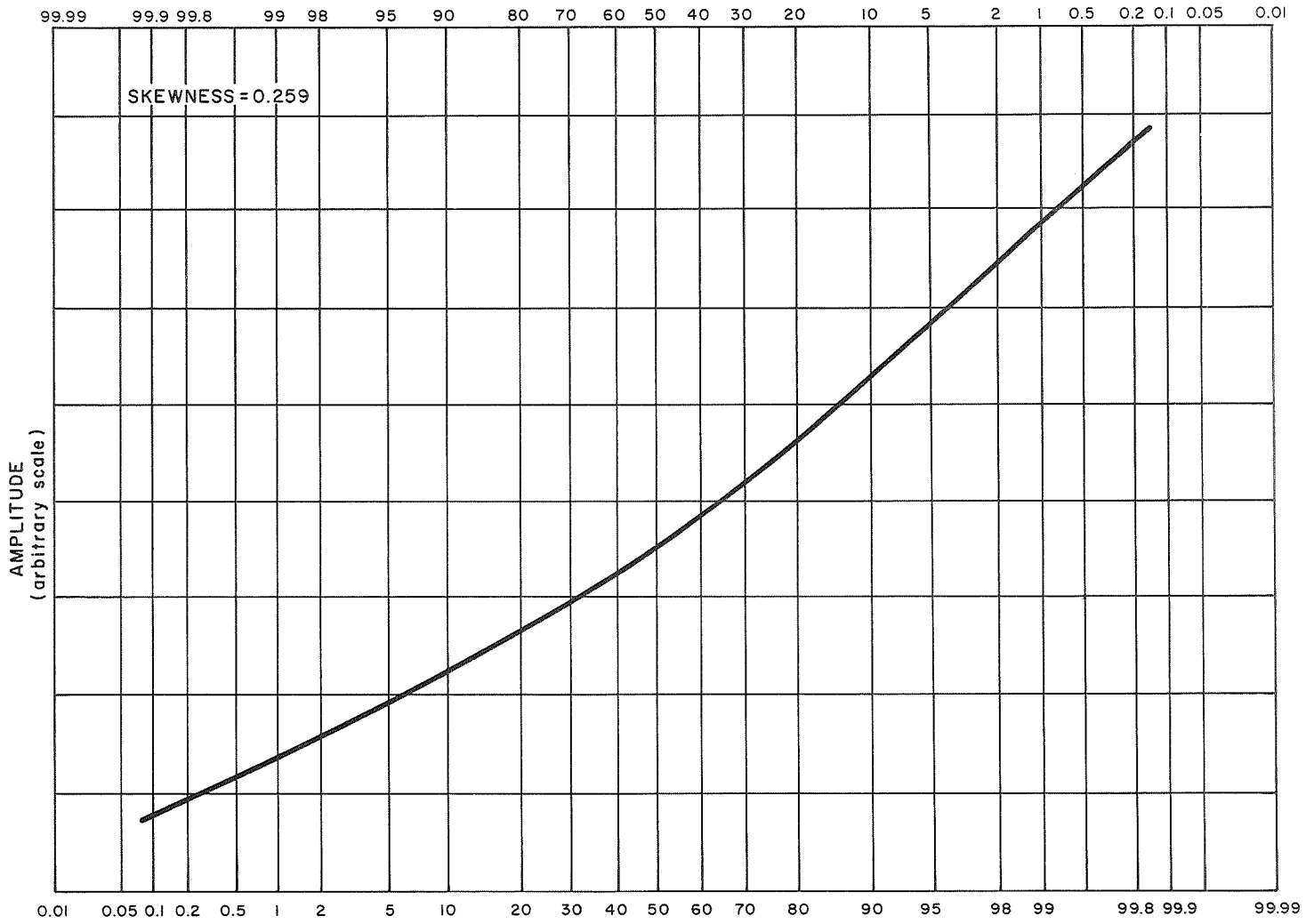

Figure 7. Probability density — skewness = 0.259.

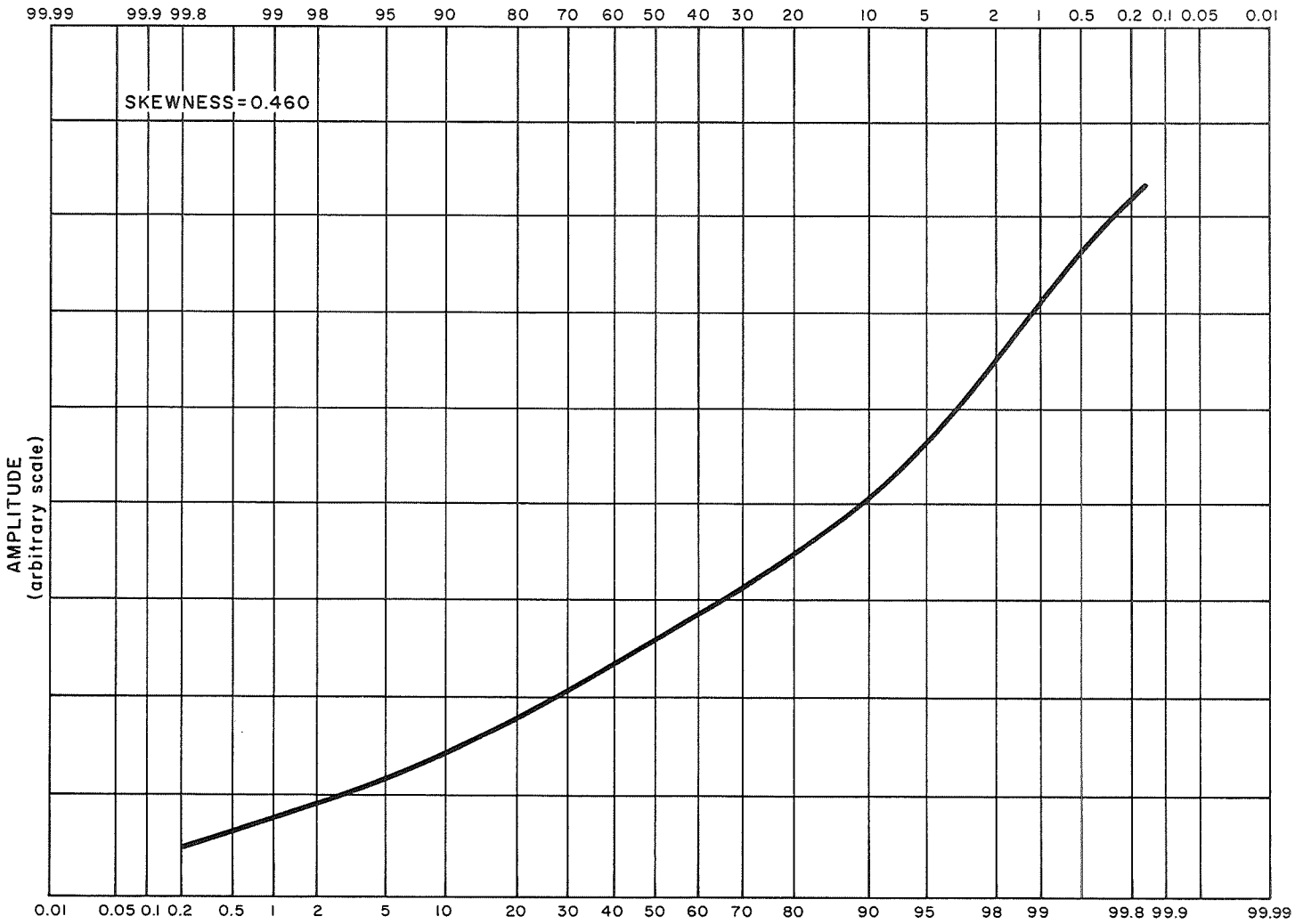

Figure 8. Probability density — skewness = 0.460.

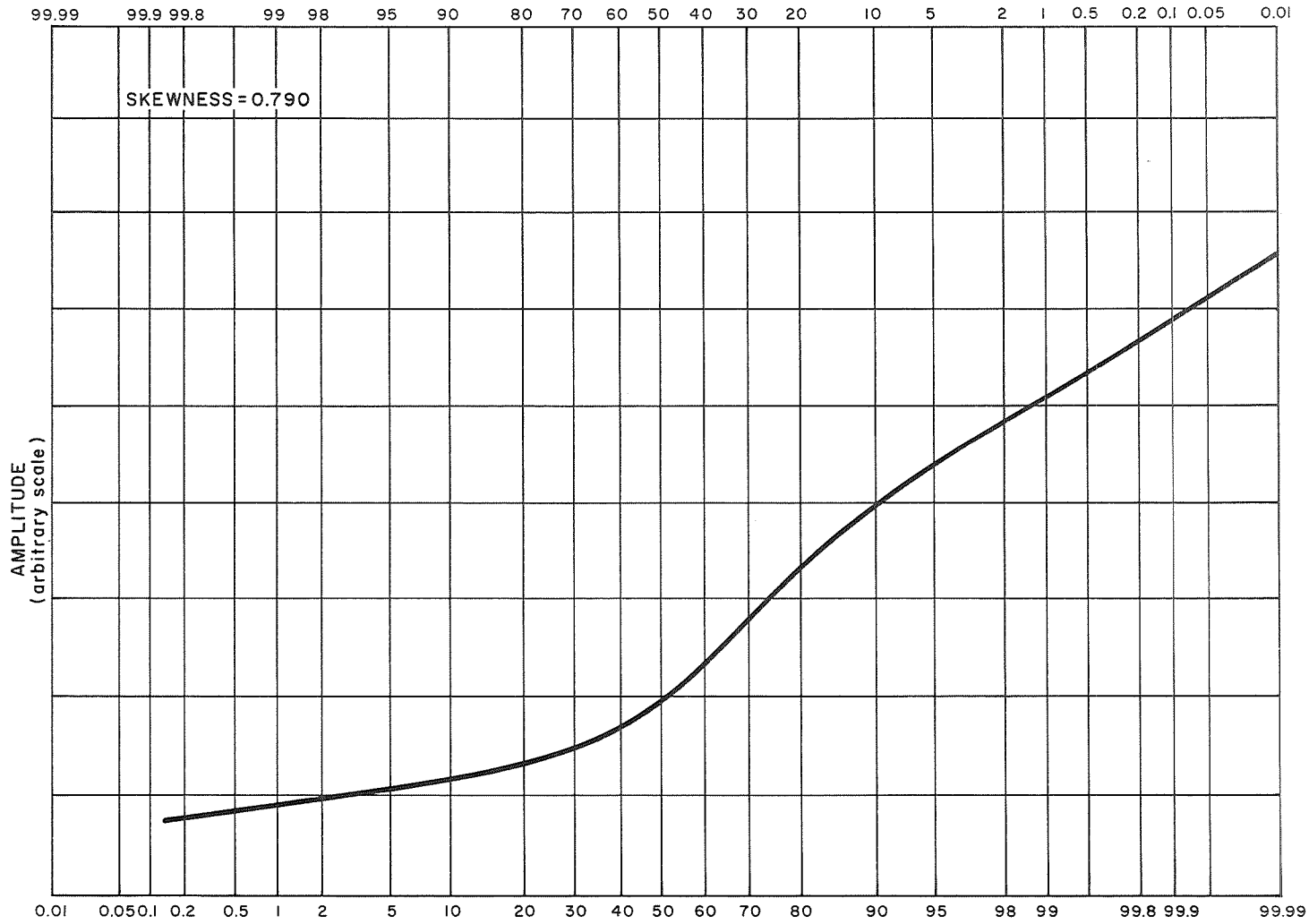

Figure 9. Probability density — skewness = 0.790.

TABLE 1. INTENSITY DISTRIBUTION VERSUS APERTURE

Aperture Size (cm)	Number of Runs				
	Total	Log-Normal	Normal	Neither	Both
2	4	2	2	0	0
4	17	13	2	1	1
6	30	10	6	13	1
8	43	12	14	11	6
10	102	33	23	37	9

tabulated. From Table 1, the 2-cm aperture runs were divided equally between normal and log-normal distributions. Since there were only 4 good runs with 2-cm apertures and since the signal was very weak for this small aperture, these results are not considered significant. The 4-cm aperture, while still reasonably small, yet large enough to give a good signal, shows a strong tendency toward log-normalcy. As the aperture increases, however, the number of runs that differ from log-normal also increases. This behavior may be caused by the effect of aperture averaging. Since this process is additive in nature, it would cause the distribution function to tend toward a normal curve. This, combined with the difficulty in distinguishing normal data from log-normal data, could lead to results of the type exhibited by our larger aperture runs.

It is believed that these results conform, within experimental accuracy, to the theoretical model for atmospheric scintillation.

STRUCTURE CONSTANT

A preliminary calculation of the atmospheric structure constant was made using equation (5) and taking the measured value of the log-amplitude variance as $C_\ell(0)$. This obviously neglects the effects of aperture averaging. Values of C_N thus obtained ranged between $1.6 \times 10^{-8} m^{-1/3}$ and $8.7 \times 10^{-8} m^{-1/3}$ for a group of runs where the aperture was varied rapidly from 2 to 10 cm. The structure constant computed from 2-cm aperture data was usually larger than that computed from 10-cm aperture data by a factor of from two to four. The time required to collect the data for such a group of runs was less than 10 minutes. As a comparison, several groups of runs were made in a similar time period holding the aperture constant. The observed variation in the structure constant for these runs was usually about 10 percent, which clearly indicates that the observed variation in structure constant was caused by aperture averaging effects and not by changes in the strength of turbulence between runs.

Using the techniques described in the previous section, we have refined our calculations of the atmospheric structure constant, allowing for the effects of aperture averaging. For the 212 segments of data that were analyzed, the values of the corrected structure constant ranged from $5.8 \times 10^{-7} m^{-1/3}$ to $9.0 \times 10^{-7} m^{-1/3}$. These values are characteristic of very strong atmospheric turbulence, which agrees with our subjective observations of the scintillation while the data were being taken.

Four typical sets of runs for various apertures are given in Table 2. As given, the variation in the structure constant is significantly reduced when the effects of aperture averaging are included. The residual variation was found to be approximately the same magnitude as the variation in scintillation between runs taken with a constant aperture over the same period of time. Thus, it may be attributable entirely to the nonstationary characteristics of the atmosphere. Note, however, that the inclusion of the aperture averaging effects has a tendency to consistently overcorrect the structure constant variation. It is impossible to be sure that this does not indicate a systematic error in recording the experimental data. On the other hand, the validity of the basic approach to the problem of aperture averaging in terms of the structure function has been questioned [12] so that it is possible that the aperture correction we have used is not exact. A third possibility is that the deep scintillation conditions under which the experimental data were collected produced saturation effects that have not been considered, since all data were taken over a constant range. In any case, this method of allowing for aperture averaging is a good approximation since the structure constant is relatively far more consistent when calculated by this method than when the effects of aperture averaging are neglected.

SCINTILLATION FREQUENCY SPECTRUM

The frequency spectrum of the scintillation has been found using the fast Fourier transform techniques described previously. Since the computation of the spectrum is a relatively time-consuming calculation, it was only performed for selected data runs that appeared to be typical. The computed spectra were very consistent, so it was believed that analysis of additional runs would yield very little additional information.

The computed spectra cover a range of frequencies from 0 (dc) to 90 Hz, the upper limit being imposed by the 180-sample-per-second sampling rate. A typical spectrum is shown in Figure 10. For the sake of clarity, only the first 20 Hz have been plotted. Above 20 Hz, the spectrum decreases linearly so that no appreciable frequency components above 40 Hz were observed.

TABLE 2. ATMOSPHERIC STRUCTURE CONSTANT (C_N IN METERS$^{-1/3}$ $\times$ 10^{-7})

Aperture Size (cm)	Run 1		Run 2		Run 3		Run 4	
	Uncor C_N	Cor C_N	Uncor C_N	Cor C_N	Uncor C_N	Cor C_N	Uncor C_N	Cor C_N
10	0.878	7.50	0.178	5.88	0.179	5.88	0.885	7.47
8	0.686	7.50	0.217	6.40	0.241	6.48	0.709	7.53
6	0.547	7.61	0.326	7.15	0.425	7.35	0.635	7.73
4	0.563	8.05	0.451	7.90	0.617	8.10	0.590	8.09
2			0.550	8.77	0.590	8.82	0.565	8.79
Mean	0.662	7.67	0.344	7.22	0.410	733	0.679	7.92
% Variation	51.7	12.9	109	40	100	40.2	47.2	16.7

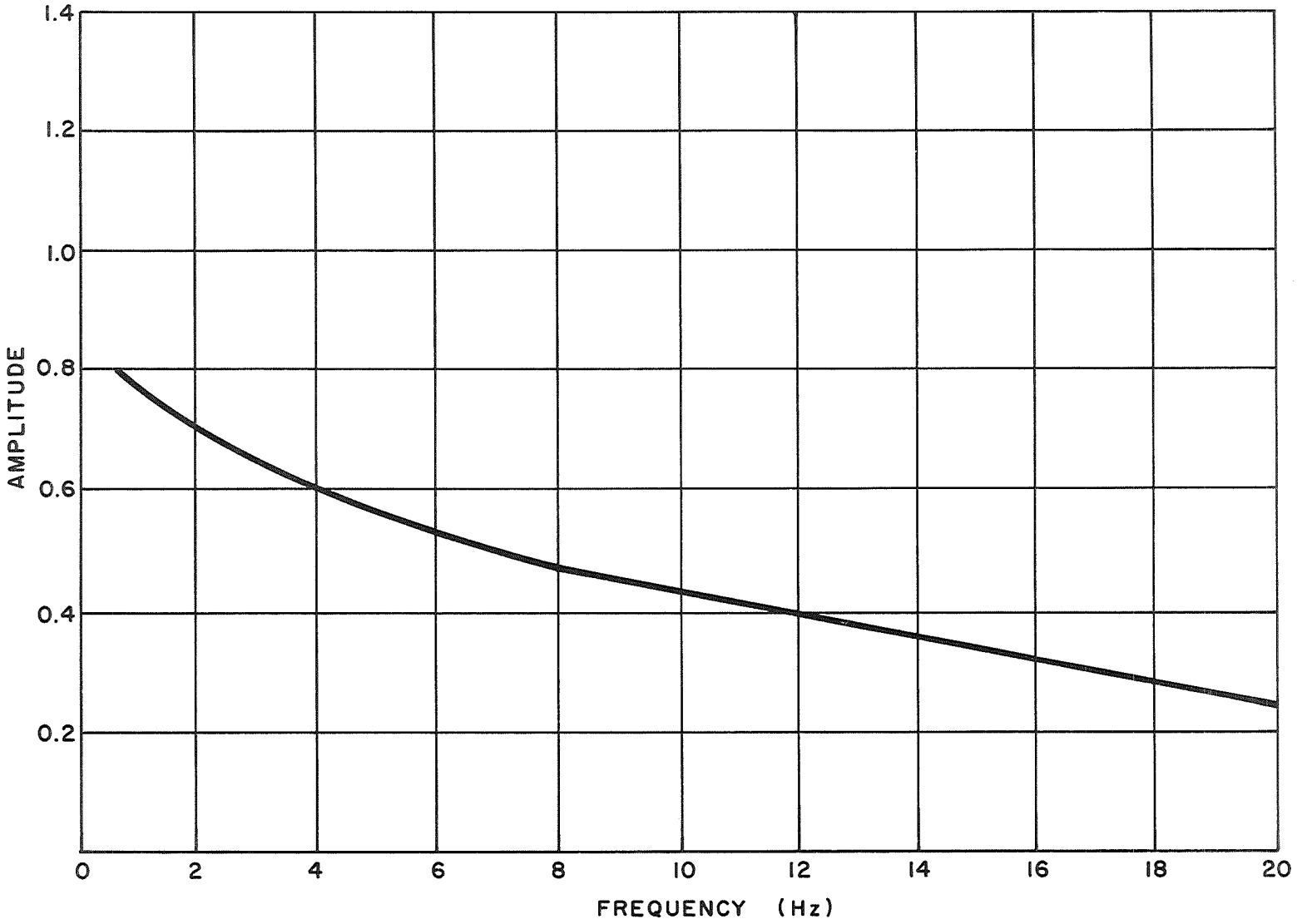

Figure 10. Amplitude spectrum.

HETERODYNE DETECTION

The effect of atmospheric turbulence on the performance of a 10-micron heterodyne system was investigated by recording both the amplitude of the 10-MHz heterodyne signal and the 1-kHz output of the FM discriminator. For all of these measurements, neither signal showed any effect attributable to atmospheric turbulence large enough to be accurately measured. Even under the conditions of deep scintillation encountered during the course of this experiment, the atmospherically induced noise was of the same order of magnitude or smaller than system noise such as detector noise and amplifier noise. Futhermore, clear voice communications were possible at this range even under the worst conditions encountered.

These results, while demonstrating the feasibility of using a heterodyne CO_2 laser system to communicate through the earth's atmosphere, were somewhat disappointing because they did not permit a quantitative measurement of the noise induced by atmospheric turbulence.

CONCLUSIONS

Measurements on the scintillation of a 10.6-micron CO_2 laser beam propagated through the earth's atmosphere indicate that to within a good approximation the scintillation and the effects of aperture averaging are correctly predicted by the Rytov solution of the wave equation. In particular, the following conclusions were reached:

(1) For small receiving apertures, the scintillation is described quite well by a log-normal distribution function. The deviations that were observed for larger receiving apertures may be caused by the effects of aperture averaging.

(2) The expression for aperture averaging given by Fried agrees approximately with the experimental data but tends to give a slightly larger value of the aperture-averaging effect than was observed. Although this may indicate an inaccuracy in the theoretical expression, a systematic error in the experimental measurements cannot be firmly ruled out.

(3) Low-frequency components of the scintillation were predominant. The magnitude of the scintillation decreases with increasing frequency. Above 40 Hz, the scintillation is negligible.

(4) The feasibility of optical heterodyne communication at 10 microns was demonstrated; however, no quantitative measurements of the atmospherically induced noise were made.

Originally, we had hoped to investigate the daily variation of the atmospheric structure constant and to correlate the magnitude of the structure constant with meterological conditions. Unfortunately, during the period when data were being collected the weather was exceptionally constant, being mostly hot and humid with light and variable winds. The consistency of the weather was undoubtedly responsible for the extremely small variation in the structure constant that was observed.

Another experiment which we had hoped to perform was to observe the effect of fog and rain on the heterodyne communication system. Because heavy morning fog is fairly common in the Huntsville area, we expected to have many opportunities for measurements in both fog and rain, but no fog or light rain occurred while data were being taken so this phase of the experiment could not be performed.

In the future, we hope to collect more data under a wider variety of conditions.

REFERENCES

1. Webb, W. E.; and Emmons, G. A.: A Survey of Atmospheric Turbulence Effects in Optical Communications Systems. MICOM Special Report, Redstone Arsenal, Alabama, August 1969.

2. Webb, W. E.: Study of Atmospheric Effects on Optical Communications. Final Report on NASA Contract NAS8-30507. University of Alabama, BER Report No. 111-70, November 1969.

3. Fried, D. L.: Optical Propagation Measurements at Lake Emmerson. Final Report, NAS1-7705, Langley Research Center, Hampton, Virginia.

4. Patton, R. B.; and Reedy, M.: Effects of Atmospheric Turbulence on Ground-to-Air Laser Beam Propagation. BRL Report 1427, Aberdeen Proving Ground, Maryland, March 1969.

5. Kerr, J. R.: Multiwavelength Laser Propagation Study II. 2nd Quarterly Report on ARPA Order No. 306, Oregon Graduate Center, Portland, Oregon, January 1970.

6. Fitzmaurice, M. W.; Bufton, J. F.; and Minott, P. O.: Wavelength Dependence of Laser Beam Scintillation. J. Opt. Soc. Am., 59, 7, 1969.

7. Mocker, H. W.: A 10.6μ Optical Heterodyne Communication System. Applied Optics, Vol. 8, No. 3, March 1969, p. 677.

8. Fried, D. L.; and Cloud, J. D.: Propagation of a Spherical Wave in a Turbulent Medium. J. Opt. Soc. Am., 56, 1966, p. 1667.

9. Fried, D. L.: Aperture Averaging of Scintillation. J. Opt. Soc. Am., 57, 1967, p. 169.

10. Fried, D. L.: Propagation of a Spherical Wave in a Turbulent Medium. J. Opt. Soc. Am., 57, 1969, p. 175.

REFERENCES (Concluded)

11. Cooley, J. W.; and Tukey, J. W.: An Algorithm for the Machine Computation of Complex Fourier Series. Math. of Comput., 19, 297, 1965.

12. Young, A. T.: Aperture Filtering and Averaging of Statistics. J. OSA, 60, 248, 1970.

APPROVAL

ATMOSPHERIC EFFECTS ON WAVE PROPAGATION AT 10.6 MICRONS

By William E. Webb, Kermit H. George, and Peter Marrero

The information in this report has been reviewed for security classification. Review of any information concerning Department of Defense or Atomic Energy Commission programs has been made by the MSFC Security Classification Officer. This report, in its entirety, has been determined to be unclassified.

This document has also been reviewed and approved for technical accuracy.

J. L. RANDALL
Chief, Applied Physics Branch

J. C. TAYLOR
Chief, Technology Division

F. B. MOORE
Director, Astrionics Laboratory

INTERNAL

DIR
DEP-T
AD-S
PM-PR-M

S&E-CSE-DIR
Dr. Haeussermann

S&E-SSL-PO
Mr. Williams

S&E-ASTR-DIR
Mr. Moore

S&E-ASTR-A
Mr. Hosenthien
Miss Flowers

S&E-ASTR-C
Mr. Swearingen

S&E-ASTR-E
Mr. Aden

S&E-ASTR-G
Mr. Mandel

S&E-ASTR-I
Mr. Duggan
Mr. Harper

S&E-ASTR-M
Mr. Boehm

S&E-ASTR-R
Mr. Taylor
Mr. Reinbolt
Dr. Randall (10)
Mr. Wyman
Mr. George
Mr. Marrero (10)

S&E-ASTR-S
Mr. Wojtalik

S&E-ASTR-ZX
A&TS-MS-IL (8)
A&TS-MS-IP (2)
A&TS-MS-H

A&TS-PAT
Mr. Wofford

A&TS-TU
Mr. Winslow

EXTERNAL

NASA Headquarters
Washington, D. C. 20546
RE — H. Anderton
RE — J. K. Meson

NASA/Goddard Space Flight Center
Greenbelt, Maryland 20771
524 — N. McAvoy

NASA/Electronics Research Center
Cambridge, Massachusetts
EOS/824 — Dr. Sherman Karp

EXTERNAL (Concluded)

Jet Propulsion Laboratory
Pasadena, California 91103
238-737 — M. Shumate

Honeywell, Inc.
Systems & Research Division
2345 Walnut St.
St. Paul, Minnesota 55113
Attn: Dr. Hans Mocker

Scientific & Technical Information
Facility (25)
P. O. Box 33
College Park, Maryland 20740
Attn: NASA Representative (S-AK/RKT)

University of Alabama
Attn: Department of Electrical
Engineering (10)
Tuscaloosa, Alabama

MSFC—RSA, Ala